Title: Investigation of Interactions of Acetylene Molecules with an Iron Nanowire and Its Effects on Mechanical Tensile Properties

Authors: Gürcan ARAL

Investigation of Interactions of Acetylene Molecules with an Iron Nanowire and Its Effects on Mechanical Tensile Properties

Gürcan ARAL[*1]

Abstract

Understanding complex atomistic-scales interactions mechanisms of reactive acetylene (C_2H_2) molecules with reactive pure iron nanowires (Fe NWs) including its effects on the tensile mechanical properties of NWs is a crucial task in nanotechnology, especially having practical significance in the mechanical reliability, durability and stability. Therefore, we performed molecular dynamics (MD) simulations based on ReaxFF reactive force field interatomic potential model to investigate the interactions of C_2H_2 molecules with surface of cylindrical pure Fe NW and its fundamental effects on the tensile mechanical deformations properties of NWs at three different strain rates. Our results reveal that the chemical energetic reactions on the free surface of cylindrical Fe NW with C_2H_2 molecules in the gas phase form $Fe_xC_yH_z$ shell layer at temperature T=300 K. The presence of $Fe_xC_yH_z$ shell layer on the free surface of NW has a significant effect on the mechanical tensile deformation mechanism of the NWs.

Keywords: acetylene, iron nanowires, molecular dynamics simulation, and reactive force field potential

[*] Corresponding Author: gurcanaral@iyte.edu.tr
[1] İzmir Institute of Technology, , İzmir, Turkey, ORCID: https://orcid.org/0000-0002-0800-0510

1. INTRODUCTION

Iron nano materials and their alloys are important engineering materials that are widely used in various nano-technological applications [1-4]. Although the nano-technological applications of Fe-containing materials are too many to be counted, this number is constantly increasing by the latest newly developed and more efficient techniques. Nanostructured Fe materials such as Fe NWs and nanorods are of scientific importance in nano-engineering applications, due to their interesting structural, chemical, physical and mechanical properties, that depend mostly on their surface structure, size and volume−surface ratios [1-5]. Generally, conductive Fe NWs and nanorods are synthesized by using many different chemical methods for different potential nano-engineering applications [1-3]. In particular, the properties of Fe NWs are strongly controlled with the formation of oxide shell layer on the free surface of the NW as a result of oxidation and any other reaction interactions with various reactive reactants [2,3,6]. More specifically, their relatively large surface−volume ratios and high affinities make the metallic pristine Fe NWs more sensitive and vulnerable to environmental influences [3,5]. For example, when the reactive metallic Fe NWs are exposed to different reactive media such as O_2, H_2O, CO_2, C_2H_2 C_2H_4, they are rapidly adsorbed and dissociated on the free surface of Fe NWs due to high affinity of these molecules to the metallic Fe NWs. Consequent formation of a native thin oxide shell layer with different limiting thickness, phase, stoichiometry, morphology, local atomic structures, and defects is inevitably covered the free surface of Fe NWs [2,3,6-12]. The formation of thin oxide layer on the free surface Fe NW naturally leads to change in the physical and chemical properties of Fe NW and consequently offers a wide range of functionalities, that are associated with its using in real-life applications [1,2,7,8]. Notably, various technological nano-engineering applications indicate that the resulting oxide shell layer on the free surface of Fe NWs plays critical roles on the mechanical performance, strength and durability of the pure Fe NW [3,5]

as well as the catalysis performance, compared with its surface in vacuum. Recent increasing demands of nano-engineering industry require a better and deeper understanding of the properties of nano Fe materials, such as the formation of oxide shell layer on the free surface of Fe NW and its effects on the corresponding mechanical tensile deformation mechanism and related properties [2,6].

We use atomistic MD simulation method based on reactive force field (ReaxFF) potential model to study a detailed systematic understanding of interactions of reactive acetylene (C_2H_2) gas molecules with cylindrical pure Fe NWs and the resulting formation $Fe_xC_yH_z$ shell layer on the free surface of NWs. Further, we determine the mechanical tensile deformation properties of the pure Fe and core-shell (Fe-$Fe_xC_yH_z$) structure NWs. In current literature, no information exits about the effects of the formation of $Fe_xC_yH_z$ shell layer on the mechanical tensile deformation mechanism and its related properties. In this respect, our MD simulations will play a very important role in filling the existing gap in current literature.

2. COMPUTATIONAL DETAILS

2.1 The reactive force field (ReaxFF) potential model and MD simulation method

MD is a computer simulation method based on the principle of calculating interactions between atoms in a physical system composed of N atoms via using potential energy function [13]. Namely, it is the numerical solution of the positions and velocities for each atom in a physical system via using Newtonian equations of motion. Newton's equation of motion is generally expressed as following:

$$m_i \frac{d^2 \mathbf{r}_i}{dt^2} = \mathbf{F}_i, \qquad (1)$$

in this equation, m_i is defined as the mass of the ith atom, $\mathbf{F}_i$ is the force acting on the ith atom and

Gürcan ARAL

Investigation of Interactions of Acetylene Molecules with an Iron Nanowire and Its Effects on Mechani...

V is the interaction potential energy function term between atoms. The first equation can be written as follows:

$$\mathbf{F}_i = -\frac{\partial V}{\partial \mathbf{r}_i}. \qquad (2)$$

Analytical potential energy function (V) describes all interactions between atoms in a physical system composed of N atoms. Therefore, it is the most important and essential input parameter for MD simulations [14]. Importantly, the quality of the simulation results produced by MD simulations depends on the precision of the potential energy function.

We carried out the MD simulations based on the ReaxFF model that was developed by van Duin et al. for Fe/C/H systems [15]. The ReaxFF interatomic potential function has successfully defined all interactions including the chemical reactions (bond formation and bond breaking) between Fe−C−H atoms in a physical system that occur during the interaction of C_2H_2 molecules with metallic Fe atoms and the mechanical deformations process [15]. This ReaxFF interatomic potential for the Fe/C/H systems includes: *i*) all ionic, covalent and metallic interactions between Fe−C−H atoms such as the core-shell ($Fe/Fe_xC_yH_z$) structure NW systems, *ii*) bond formation and breaking between Fe−C−H atoms, and also *iii*) charge variation between atoms whenever atoms change their local environment. These necessary considerations allow the MD simulations to accurately describe properties of the physical system. In other words, the realistic ReaxFF potential model allows us to accurately simulate the scientific, technological and nano-engineering problem of uniaxial mechanical tensile deformation mechanism and predict related properties of the core-shell ($Fe/Fe_xC_yH_z$) structure NWs [15].

2.2 Simulation set up and details

We begin with briefly describing the construction of [001] −oriented cylindrical pure Fe NW in the middle of a MD box. Iron atoms have a body centered cubic (BCC) unit crystal lattice structure with a unit length (a lattice constant) of 2.86 Å. First, we took 70 x 70 x 50 unit lattice cells in the x, y and z directions, respectively. As a result, a rectangular MD box consisting of only Fe atoms was created with dimensions of 20.041 x 20.041 x 14.315 nm in the x, y and z directions, respectively. Then, Fe atoms with radial distance from the middle of the MD box in the x-y plane greater than 5.0 nm that were deleted. Thus, we created a cylindrical pure Fe NW with a length of 14.315 nm and a diameter of 5.0 nm, containing 24,050 Fe atoms in vacuum, as seen in Fig. 1(a). The pure Fe NW is parallel to the z-axis. The uniaxial tensile loading is also applied in z-direction.
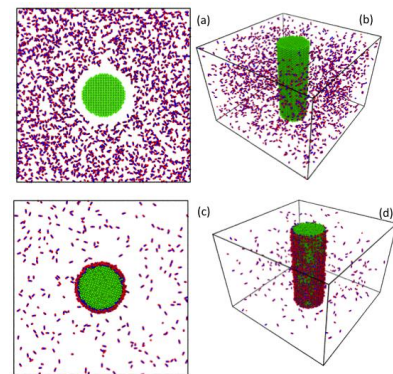

Figure 1 At the beginning of the simulation, a cylindrical pure Fe NW with a 5.0 nm diameter and 14,315 nm length was placed in the MD box. Then, 2,000 C_2H_2 molecular were dispersed randomly in the MD box, as shown in (a) sectional view and (b) side view along the z-axis. At t=3.3 ns, the formation of $Fe_xC_yH_z$ shell layer on the free surface of pure Fe NW is shown in (c) sectional view and (d) side view along the z-axis. The green, blue, and red colors indicate Fe, C and H atoms, respectively.

To study the interaction of C_2H_2 acetylene molecules with cylindrical pure Fe NW, randomly oriented 2,000 C_2H_2 molecules were inserted at a distance of 6 Å from the free surface of [001] −oriented cylindrical pure Fe NW within the MD box. The simulations were carried out using (NVT) Nose Hoover thermostats at a

Gürcan ARAL

Investigation of Interactions of Acetylene Molecules with an Iron Nanowire and Its Effects on Mechani...

temperature of 300 K [16]. The equation of motions were integrated numerically with velocity Verlet algorithm using a time step of 0.25 fs. Complex interactions processes occur instantaneously at the free surface of NW when it comes in contact with the C_2H_2 molecules at T=300K. As a result of reactive interactions, the $Fe_xC_yH_z$ shell layer was formed on the free surface of NW. Later, we deleted the C_2H_2 molecules from the MD simulation box that did not interact with the NW, that is, did not bond with the Fe atoms of NW. The snapshots in Figure 1 clearly show the initial configurations of the cylindrical pure Fe NW in the environment of C_2H_2 molecules and the final formation of the core-shell (Fe/$Fe_xC_yH_z$) structures. We used the Ovito−open visualization tool to obtain detailed atomistic level information of the formation of the core-shell (Fe/$Fe_xC_yH_z$) structures [17].

Prior to applying the uniaxial mechanical tensile load on the cylindrical pure Fe and core/shell (Fe/$Fe_xC_yH_z$) structure NWs, the configurations of all NWs were first relaxed to minimum energy positions using conjugate gradient method. Then, they were thermalized at 300 K under the Nose Hoover thermostats. Next, they were relaxed to be in equilibrium using Nosé-Hoover isothermal-isobaric (NPT) thermostats at T=300K and the zero pressure along the z-axis [18]. Finally, an external mechanical tensile load along [001] direction at three different tensile strain rates ($1x10^8$ s^{-1}, $5x10^8$ s^{-1} and $1x10^7$ s^{-1}) were applied on the well-equilibrated NWs under the canonical (NVT) ensemble at 300 K [16]. Periodic boundary conditions were applied in the loading direction while free surface was used in the x and y direction. We obtained the average engineering stress by correcting the Virial stress equation with the original volume of the NWs [13]. All uniaxial mechanical tensile loads were applied to NWs until they reached ~16% elongation. The total simulation time for the formation of $Fe_xC_yH_z$ layer on the free surface of NW and the tensile test was 3.3 and 1.5 ns, respectively. All MD simulations were performed via using LAMMPS (Large-scale Atomic/Molecular Massively Parallel Simulator) open source codes [19].

3. RESULTS AND DISCUSSIONS

3.1 Reaction of acetylene molecules with Fe NW and formation of the $Fe_xC_yH_z$ shell layer

We simulated interaction events that occurred with C_2H_2 molecules on the free surface of cylindrical pure Fe NW at temperature T=300K in the simulation of 3.3ns duration. In this reactive interaction process, 1,730 out of total 2,000 C_2H_2 molecules in the gas phase interacted with the pure Fe NW and consequently, a thin $Fe_xC_yH_z$ shell layer was formed on the free surface of NW. Namely, the pure Fe NW transforms into core/shell (Fe/$Fe_xC_yH_z$) structure, as a result of complex interaction of C_2H_2 molecules with Fe atoms a taking place on the free surface of the pure Fe NW. Snapshots as seen in the Figure 2 confirm that the initial formation of the $Fe_xC_yH_z$ shell layer around the free surface of Fe NW occurs rapidly and increases with time due to high affinity of Fe atoms to C_2H_2 molecules. Almost all C_2H_2 molecules interact directly with the Fe atoms around the reactive sites of the free surface of NW and consequently combine to form a bond between atoms. Importantly, formation and growth process of the $Fe_xC_yH_z$ shell layer on the free surface in C_2H_2 molecular environment is driven by combination of local chemical and physical reactions that occur around the free surface of reactive pure Fe NW and develop independently from each other.
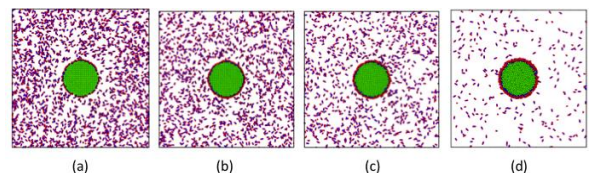

Figure 2 The pure Fe NW was initially placed in a randomly oriented and dispersed 2,000 C_2H_2 molecular environments. The formation of the $Fe_xC_yH_z$ shell layer on the surface of pristine Fe NW is shown from sectional view along the axis at (a) 0.00875 ns, (b) 0.05 ns, (c) 0.25 ns and (d) 3.3 ns. The green, blue, and red colors indicate Fe, C and H atoms, respectively.

Gürcan ARAL

Investigation of Interactions of Acetylene Molecules with an Iron Nanowire and Its Effects on Mechani...

We analyzed the bond lengths between C−H and C−C atoms in the resulting formation of $Fe_xC_yH_z$ shell layer using the radial pair distribution functions (RDF), as seen in Figure 3. During the interaction process of C_2H_2 molecules with Fe atoms, CH ions (fragments) were formed on the free surface due to C−C bond breakage within C_2H_2 molecules. Specifically, the two peaks in Figure 3 (b), which are ∼ 1.15 and ∼ 1.28 Å, indicates the C−C bond breaking between the constituent atoms of the C_2H_2 molecule. On the other hand, the bond lengths and distributions formed between C−H atoms in Figure 3 (a) indicate that some C_2H_2 molecules interact with the Fe NW to maintain their molecular structure and also to form of CH fragments. During the reaction process, CH and Fe ions partially diffuse inward and outward around the reaction region of the NW, respectively. These corresponding diffusions in tandem with the charges transfer and bonds formation between the atoms cause the formation of the $Fe_xC_yH_z$ shell layer on the free surface of NW. As time progresses during the interaction process, the resulting $Fe_xC_yH_z$ shell layer grows rapidly and becomes thicker causing the interaction kinetics to slow down. The development of $Fe_xC_yH_z$ shell layer gradually blocks diffusions paths of ions also, the interaction activity including dissociation of C_2H_2 molecules and the rate of penetration of ions decrease with the growth of the $Fe_xC_yH_z$ shell layer. In addition, the molecular pressure of C_2H_2 molecules is decreased by adsorption C_2H_2 molecules. The resulting interactions, the partial ionic diffusions and the bond formations, and the charges transfer between atoms on the free surface causes significant changes of the local atomic structure of free surface of NW leading to the formation of $Fe_xC_yH_z$ shell layer over time. As the formation of the $Fe_xC_yH_z$ shell layer thickness increases, the concentration of C and H atoms around the free surface of NW increases over time, indicating a successful formation of bonds between atoms. As a result, the pure Fe NW transforms into the core/shell $(Fe/Fe_xC_yH_z)$ structure NW. Also, the developing $Fe_xC_yH_z$ shell layer on the free surfaces provides a physical separation between the pure Fe NW and reactive C_2H_2 molecules, thus the thin $Fe_xC_yH_z$

shell layer acts as a natural diffusion barrier for reactive C_2H_2 molecules over time.
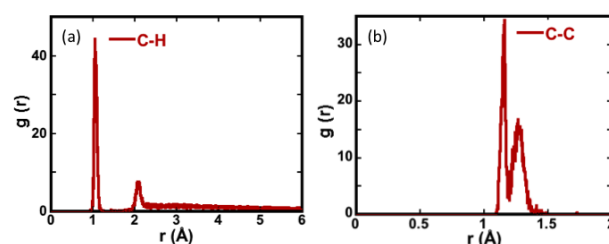

Figure 3 Radial pair distribution functions between a) C-H and b) C-C atoms are shown in the resulting formation of $Fe_xC_yH_z$ layer in the active regions close to the free surface of the cylindrical metallic Fe NW as a result of the interaction process.

Kayastha et al. observed simultaneous dissociative adsorption of C_2H_2 molecules on Fe surface, eventually leading to the formation of amorphous shell layer on the free surfaces of Fe nanoparticles that gradually prevented further contact of C_2H_2 molecules with Fe nanoparticles [11]. Also, the C_2H_2 molecules are decomposed into two CH fragments as a result of dissociative adsorption of C_2H_2 molecules on the free surface of Fe nanoparticles. In particular, they revealed that CH fragments are formed by breaking the bonds between C=C atoms in a C_2H_2 molecule. Moreover, metallic Fe atoms interact with C_2H_2 molecules to form of CH−Fe bonds, exhibiting preferentially down orientation of C atoms to the free surface. Lee et al. investigated interaction of C_2H_2 molecules on Fe [001] surface through first-principles electronic structure calculation [10]. They indicated that dissociation process involves the C−C bond breaking between constituent atoms of the C_2H_2 molecule to form CH fragments. Moreover, absorption of C_2H_2 molecules on the free surface of NW is a highly exothermic process that creates conditions for outward diffusion of Fe and inward diffusion of CH ions.

We investigated the thickness of formed $Fe_xC_yH_z$ shell layer by analyzing the atomic radial number density distribution profiles of Fe, C and H atoms per unit volume. Figure 4 highlights the total number of C_2H_2 molecules interact with pure Fe NW during the interaction process. Specifically, analysis of the atomic radial number density distribution profiles of Fe, C and

Gürcan ARAL

Investigation of Interactions of Acetylene Molecules with an Iron Nanowire and Its Effects on Mechani...

H atoms per unit volume indicates the outward diffusion of Fe ions and the inward diffusion of CH ions. Also, the positions, widths, and densities of the atomic radial number density distribution profiles of atoms reveal that the formed $Fe_xC_yH_z$ shell layer on the free surface of NW is not very uniform, and its density depends on the radial length. As a result interaction at time=3.3 ns, the average radius of the cylindrical pure Fe NW increases from r=~2.50 nm to r=~3.0 nm. Also the average thickness of the formed $Fe_xC_yH_z$ shell layer is ~0.7 nm as a result of the diffusion of CH ions, and also the attachment of the C_2H_2 molecules to the free surface of NW by making various bonds among Fe, C and H atoms. Moreover, Fe atoms diffused from the metallic core (r=~2.50 nm) to outward (r=~2.7 nm). As expected, these ionic diffusions happen along with the charges transfer between atoms. The formation of $Fe_xC_yH_z$ shell layer on the free surface of NW leads to significant local atomic structure modulation and morphology changes on the free surface of NW including the radial expansion of ~18.4% and volume expansion of ~65.0%. In other words, the bonds formed between the atoms result in the formation of the $Fe_xC_yH_z$ layer on the surface that causes significant changes in the surface chemical and physical properties of the NW including morphology and diameter of NW.
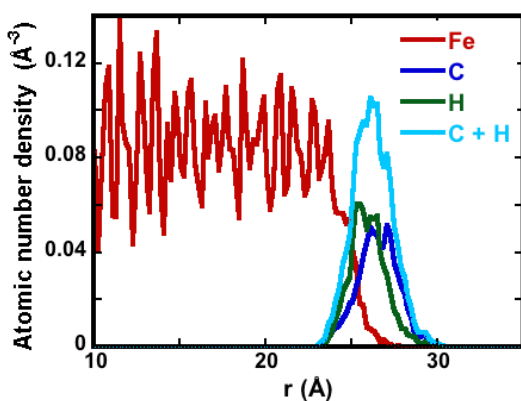

Figure 4 The atomic radial number density distribution profiles of the core/shell (Fe/$Fe_xC_yH_z$) structure are shown for C (dark blue), H (green) and C+H (blue) atoms. The atomic radial number density profiles were created by using 0.5 Å intervals along radial direction.

3.2 Formation of $Fe_xC_yH_z$ shell layer influencing the uniaxial tensile deformation properties

We performed external uniaxial mechanical tensile loading on cylindrical pure and core-shell (Fe/$Fe_xC_yH_z$) NWs at temperature T=300K and three different strain rates (1×10^8 s^{-1}, 5×10^8 s^{-1} and 1×10^7 s^{-1}). We analyzed the effects and changes of mechanical tensile deformation behaviors and corresponding properties of the pure and the layer-shell (Fe/$Fe_xC_yH_z$) NWs. Here, the pure Fe NW was taken as reference in order to compare how much the relevant properties and constants of the NW changed after the formation of $Fe_xC_yH_z$ shell layer on the free surface of NW.

As seen clearly in Figure 5, the engineering average tensile stress-strain curves of the pure and $Fe_xC_yH_z$ coated Fe NW indicate that they have notably different tensile mechanical properties and constants, depending on the external applied uniaxial tensile strain and the existence of $Fe_xC_yH_z$ shell layer. Moreover, the change of average engineering stress-strain curves show a significant reduction in strength of the $Fe_xC_yH_z$ layer-coated Fe NW as compared to the pure counterpart. But, the overall deformation trends of the average engineering stress-strain curves are very similar for all NWs [7,8,20]. Moreover, the existence of the $Fe_xC_yH_z$ shell layer leads to significantly reduce the elastic strain limit (elongation of tensile elasticity) of NW as well as the average maximum stress (yield stress) to onset of the tensile plasticity. The average engineering stress-strain curves of all NW show three different tensile deformation regimes: linear elastic, non-linear elastic and plastic deformation regime [7,8]. Specifically, the average stress profiles for all NWs, whether pure or $Fe_xC_yH_z$ shell layer coated Fe NWs, experience a sudden drop in stress after reaching their yield stress values, indicating that the NWs subsequently undergo tensile plastic deformation. Also, the average engineering stress-strain curves reveal that pure Fe NW exhibits a higher mechanical tensile resistance to onset of the tensile plasticity as

Gürcan ARAL

Investigation of Interactions of Acetylene Molecules with an Iron Nanowire and Its Effects on Mechani...
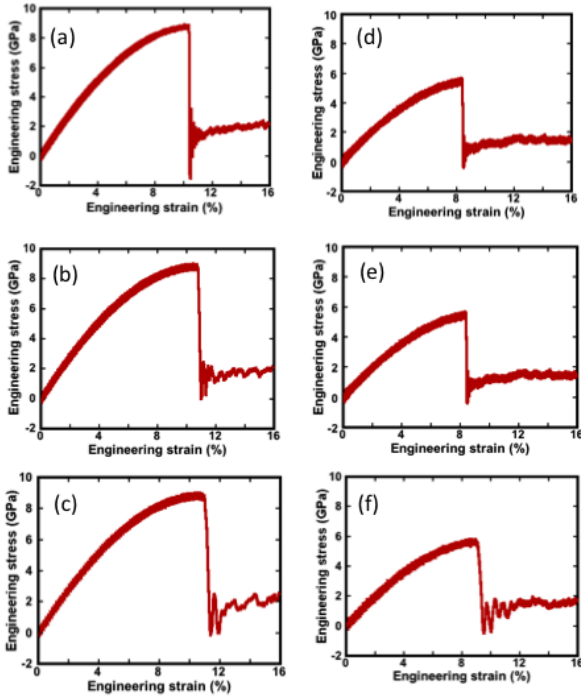
compared to the core-shell ($Fe/Fe_xC_yH_z$) structure counterpart.

Figure 5 The average engineering tensile stress-strain curve for pure Fe NW is shown at different strain rates of: a) $1x10^8s^{-1}$, b) $5x10^8s^{-1}$ and c) $1x10^7s^{-1}$ values. On the other hand, the engineering average tensile stress-strain curve for the core-shell structure ($Fe/Fe_xC_yH_z$) NW is shown at different strain rates of: d) $1x10^8s^{-1}$, e) $5x10^8s^{-1}$ and f) $1x10^7s^{-1}$ values.

In the non-linear elastic regime, the flow tensile stress increases gradually up to the yield stress level with increasing external applied tensile strain, and then followed by a sudden flow stress drop, indicating release of elastic energy. The tensile plastic deformation occurs a relatively low stress with fluctuating stress values around 1.0-2.0 GPa. In the meantime, the NWs beyond the yield stress continue their tensile plastic deformation with the increase of tensile stress at the partially low stress values. Specifically, twinning is a main plastic deformation mechanism. Also, it is the tensile plastic stress carrier in the plastic deformation region, leading to continued plastic deformation at partially low flow tensile stress [7,8,20]. The twinning is predominantly controlled by the relative ease of creation of defects and the propagation of displacement activities along the twin boundaries. The yield stress values for the pure Fe NWs are ~8.7 GPa for three different strain rates ($1x10^8s^{-1}$, $5x10^8s^{-1}$ and $1x10^7s^{-1}$). Corresponding to these tensile yield stress values, the yield strain values occur at ~10.4, ~10.8 and ~11.1% at the strain rates of $1x10^8s^{-1}$, $5x10^8s^{-1}$, and $1x10^7s^{-1}$, respectively. The average tensile yield stress values remain the same, but the elastic limit values depend highly on the applied external strain rates. On the other hand, the yield tensile stress values for the Fe NW covered with the $Fe_xC_yH_z$ shell layer are ~5.5 GPa and the yield strain values are ~8.4, ~9.6 and ~9.1% at three different strain rates of $1x10^8s^{-1}$, $5x10^8s^{-1}$, and $1x10^7s^{-1}$, respectively. The yield stresses for $Fe_xC_yH_z$-coated Fe NWs are approximately ~37% lower than that of their pure counterparts. Notably, our result implies that the existence of defects and interstitial impurities in the $Fe_xC_yH_z$ shell layer on the free surface of NW leads to significant decrease in the tensile yield stress value to onset tensile plasticity. The yield stress for the pure Fe NW indicates a relatively higher stress value required to initiate tensile plasticity as compared to the $Fe_xC_yH_z$-coated counterpart. Importantly, the applied external strain rates have a relatively negligible effect on the corresponding required yield tensile stress values to initiate the tensile plasticity; but it has a strong effect on the elastic elongation limits. However, variations of the engineering average stress-strain curves beyond the elastic limit, i.e. in the tensile plastic region, are only little sensitive to the existing of $Fe_xC_yH_z$ shell layer and strain rates.

The tensile yield stress and strain values depend strongly on the surface-related correlations and competitions, especially, the initial defect structures on the free surface of NWs. Here, the existence of the $Fe_xC_yH_z$ shell layer on the free surface of Fe NW leads to reduction of the tensile yield stress. This is because of the existence of defects on the free surface of NWs due to rapid formation of $Fe_xC_yH_z$ shell layer that naturally facilitates the initiation of plastic deformation in the Fe NWs. Importantly, the formed $Fe_xC_yH_z$ shell layer significantly reduces the tensile yield stress and also limit value of the elastic elongation limit, accelerating the onset of tensile plasticity.

Gürcan ARAL

Investigation of Interactions of Acetylene Molecules with an Iron Nanowire and Its Effects on Mechani...

In our literature research, there are only a few studies related to the deformation behavior of pure Fe NWs as a function of the applied external strain rates. Our results are consistent with our previous research and other's studies of tensile mechanical deformation of Fe NWs [20]. For example, Li and Han investigated tensile deformation behaviors of [001] −oriented single crystal Fe NW for different temperatures (900 K − 0.1 K) and strain rates ($1.25 \times 10^7 s^{-1}$ − $1.25 \times 10^{10} s^{-1}$) by using MD simulations [21]. They found that Young's modulus and yield stress value were independent of the applied strain rates at the low-temperature, but these two properties decrease with increasing temperature. In addition, the Fe NWs are deformed mainly by twinning during the tensile plastic deformation region. Zhao and Liu studied the effects of strain rates ($1 \times 10^9 s^{-1}$ − $5 \times 10^6 s^{-1}$) on tensile mechanical deformation behaviors and related properties for pure copper (Cu) NWs [22]. In their study, they observed that corresponding tensile stress-strain curves in the tensile elastic regions are completely identical for all applied strain rates. However, they observed that the strain rate affects the tensile plastic deformation mechanism. Xie et al. investigated the uniaxial tensile plastic deformation mechanism of metallic [110]-oriented Fe NWs using MD simulation method [23]. Moreover, the tensile deformation of Fe NWs in the linear elastic region is completely insensitive to the strain rate. Also, they observed that the flow tensile stress drops suddenly to approximately 2.5 GPa flow stress value after reaching the yield stress value; indicating that plastic deformation starts at the same time.

In our study, we shown that the active C_2H_2 molecules interact rapidly with the Fe atoms on the free surface of NW, and consequently the pure Fe NW transforms into the core/shell ($Fe/Fe_xC_yH_z$) structure. We observed that the core/shell ($Fe/Fe_xC_yH_z$) structure NW has different tensile mechanical properties and related constant, as compared to the pure counterpart. Particularly, the onset of tensile plastic deformation of NWs is facilitated due to the existence of $Fe_xC_yH_z$ shell layer on the free surface of NW. Also, the pure Fe NWs can withstand relatively higher tensile yield stress and strain than that of the $Fe_xC_yH_z$ shell layer counterparts under externally applied mechanical tensile load. Importantly, the yield stress values are independent of the strain rates.

4. CONCLUSIONS

We investigated the tensile mechanical deformation properties of the pure and the $Fe_xC_yH_z$ layer coated Fe NWs and the related mechanical constants at T = 300 K for three different strain rates ($1 \times 10^7 s^{-1}$, $5 \times 10^8 s^{-1}$ and $1 \times 10^8 s^{-1}$). As a result; the $Fe_xC_yH_z$ layer formed on the free surface of the cylindrical pure Fe NW has a detrimental effect on tensile mechanical properties of pure Fe NW such as reduction of the mechanical tensile strength. We observed similar tensile elastic and plastic deformation behaviors under externally applied constant strain rates for all NW, except the yield stress and strain values that corresponds to the onset tensile plastic deformation. In comparison, the formed $Fe_xC_yH_z$ shell layer has a significant effect on the tensile mechanical deformation performance and related properties of the pure Fe NWs. In particular, the existence of $Fe_xC_yH_z$ shell layer on the free surface of NW significantly reduces the tensile stress and strain values required onset of the tensile plastic deformation.

In addition, it is of great importance to understand the tensile mechanical deformation mechanism of core-shell ($Fe-Fe_xC_yH_z$) NWs at different strain rates. We believe that our simulation results are very important and provide valuable contributions to many questions related to interaction of C_2H_2 molecules with pure Fe NW and its resulting effects on the tensile mechanical deformation related properties. For example, our estimation of the relevant tensile mechanical properties and constant will be of great interest in the future.

The Declaration of Conflict of Interest/Common Interest

No conflict of interest or common interest has been declared by the author.

The Declaration of Ethics Committee Approval

The author declares that this document does not require an ethics committee approval or any special permission.

The Declaration of Research and Publication Ethics

The author of the paper declares that he complies with the scientific, ethical and quotation rules of SAUJS in all processes of the article and that he does not make any falsification on the data collected. In addition, he declares that Sakarya University Journal of Science and its editorial board have no responsibility for any ethical violations that may be encountered, and that this study has not been evaluated in any academic publication environment other than Sakarya University Journal of Science.

REFERENCES

[1] A. Ali, H. Zafar, M. Zia, I.U. Haq, A.R. Phull, J.S. Ali, and A. Hussain, "Synthesis, characterization, applications, and challenges of iron oxide nanoparticles," Nanotechnology, Science and Applications, vol. 9, pp. 49–67, 2016.

[2] M. Krajewski, K. Brzozka, W.S. Lin, H.M. Lin, M. Tokarczyk, J. Borysiuk, G. Kowalskia, and D. Wasik, "High temperature oxidation of iron-iron oxide core-shell nanowires composed of iron nanoparticle," Physical Chemistry Chemical Physics, vol. 18, pp. 3900–3909, 2016.

[3] K. Gandha, J. Mohapatra, M.K Hossain, K. Elkins, N. Poudyal, K. Rajeshwarb, and J.P. Liu, "Mesoporous iron oxide nanowires: synthesis, magnetic and photo catalytic properties," RSC Advances, vol. 93, pp. 90537–90546, 2016.

[4] P. Landau, Q. Guo, P. Hosemann, Y. Wang, and J. R. Greer, "Deformation of as-fabricated and helium implanted 100 nm-diameter iron nano-pillars," Materials Science and Engineering: A, vo. 612, pp. 316–325, 2014.

[5] B. R. S. Rogne and C. Thaulow, "Strengthening mechanism of iron micro pillars," Philosophical Magazine, vol. 95, pp. 1814–1828, 2015.

[6] B. Jeon, Q. V. Overmeere, A. C. T. van Duin, and S. Ramanathan, "Nano scale oxidation and complex oxide growth on single crystal iron surfaces and external electric field effects," Physical Chemistry Chemical Physics, vol. 15, pp. 1821, 2013.

[7] G. Aral, Y. J. Wang, S. Ogata, and A. C. T. van Duin, "Effects of oxidation on tensile deformation of iron nanowires: Insights from reactive molecular dynamics simulations," Journal of Applied Physics, vol. 120, no 13, pp. 135104–1–14, 2016.

[8] G. Aral, M. M. Islam, Y. J. Wang, S. Ogata, and A. C. T. van Duin, "Oxyhydroxide of metallic nanowires in a molecular H2O and H2O2 environment and their effects on mechanical properties," Physical Chemistry Chemical Physics, vol. 20, no. 25, pp. 17289–17303, 2018.

[9] T. Pan, "Quantum chemistry-based study on iron oxidation at the iron-water interface: An X-ray analysis aided study,"

Gürcan ARAL

Investigation of Interactions of Acetylene Molecules with an Iron Nanowire and Its Effects on Mechani...

Chemical Physics Letters, vol. 511, pp. 315–321, 2011.

[10] G. D. Lee, S. Han, J. Yu, and J. Ihm, "Catalytic decomposition of acetylene on Fe [001]: A first-principles study," Physical Review B, vol. 66, pp. 081403–081407, 2002.

[11] V. Kayastha, Y. K. Yap, S. Dimovski, and Y. Gogots, "Controlling dissociative adsorption for effective growth of carbon nanotubes," Applied Physics Letters, vol. 85, no. 15, pp. 3265–3267, 2004.

[12] F. G. Sen, A. T. Alpas, A. C. T van Duin, and Y. Qi, "Oxidation-assisted ductility of aluminum nanowires," Nature Communications, vol. 5, pp. 3959–3968, 2014.

[13] M. P. Allen and L. J. Tildesley, Computer Simulation of Liquids. New York, USA, Oxford University Press, 1987.

[14] K. I. Nomuro, R. K. Kalia, A. Nakano, and P. Vashishta, "A scalable parallel algorithm for large-scale reactive force field-field molecular dynamics simulations," Computer Physics Communications, vol. 178, pp. 73–87, 2008.

[15] M. M. Islam, C. Zou, A. C. T. van Duin, and S. Raman, "Interactions of hydrogen with the iron and iron carbide interfaces: a ReaxFF molecular dynamics Study," Physical Chemistry Chemical Physics, vol. 18, pp. 761–771, 2016.

[16] G. J. Martyna, M. L. Klein and M. Tuckerman, "Nose-Hoover chains: the canonical ensemble via continuous Dynamics," Journal of Chemical Physics, vol. 97, pp. 2635–2643, 1992.

[17] A. Stukowski, "Visualization and analysis of atomistic simulation data with OVITO– the Open Visualization Tool," Modeling and Simulation in Materials Science and Engineering, vol. 18, pp. 015012, 2010.

[18] G. J. Martyna, D. J. Tobias and M. L. Klein, "Constant pressure molecular dynamics algorithms," Journal of Chemical Physics, vol. 101, no. 5, pp. 4177–4189, 1994.

[19] S. Plimpton, "Fast Parallel Algorithms for short-Range Molecular Dynamics," Journal of Computational Physics, vol. 117, pp. 1–19, 1995.

[20] C. J. Healy, and G. J. Ackland, "Molecular dynamics simulations of compression-tension asymmetry in plasticity of Fe nanopillars," Acta Materialia, vol. 70, pp. 105–112, 2014.

[21] L. Li, and M. Han, "Molecular dynamics simulations on tensile behaviors of single-crystal bcc Fe nanowire: effects of strain rates and thermal environment," Applied Physics A, Materials Science & Processing, vol. 123, no 450, pp. 1–7, 2017.

[22] L. Y. Zhao, and Y. Liu, "The influence mechanism of the strain rate on the tensile behavior of copper nanowire," Science China Technological Sciences, vol. 62, pp. 2014–2020, 2019.

[23] H. Xie, T. Yu, W. Fang, F. Yin and D. F. Khan, "Strain-rate-induced bcc-to-hcp phase transformation of Fe nanowires," Chinese Physics B, vol. 25, no. 12, pp. 126201–126207, 2016